

## Four-Arm Oligonucleotide Ni(II)–Cyclam-Centered Complexes as Precursors for the Generation of Supramolecular Periodic Assemblies

Kristen M. Stewart and Larry W. McLaughlin\*

Contribution from the Department of Chemistry, Merkert Chemistry Center, Boston College, 2609 Beacon Street, Chestnut Hill, Massachusetts 02467-3801

Received July 21, 2003; E-mail: mclaughl@bc.edu

**Abstract:** The development of a multiarm metal-centered DNA building block as a precursor for the construction of supramolecular assemblies has relied upon the preparation of a Ni(II)–1,4,8,11-tetrazacyclotetradecane ligand (cyclam) functionalized with four linkers. This complex can be incorporated into a support-bound DNA sequence and the remaining three linkers can then be elongated by DNA synthesis. The result is a Ni(II)–cyclam complex tethering four 20-mer DNA strands. This building block, designed to be tetrahedral in nature, can in principle be used to form tetrahedral assemblies. These assemblies can be designed to be of known size and composition or permitted to grow into complexes of essentially infinite size, ideally the macroscopic version of a crystal.

In principle, it is possible to obtain many geometric arrangements from the hybridization of building blocks tethering multiple DNA sequences. A simple “hub” containing two DNA sequences could be used to construct linear arrays, while one containing three arms could result in a largely planar assembly. We herein describe the first example of building blocks, each composed of a metal-centered hub tethering four DNA arms, as precursors for the assembly of three-dimensional mesoscale periodic assemblies.

A mesoscale periodic lattice, one that could be essentially infinite in size, would be composed of arms with dimensions of tens of nanometers or more, and the geometric arrangement of the arms would define pores that could host guest molecules of macroscale sizes. Double-stranded DNA is potentially an optimal choice for the construction of such periodic arrays as suggested by Seeman<sup>1,2</sup> since it can assemble into long and fairly rigid helices, based simply on sequence complementarity. The double-stranded DNA helix, a common biological structure, could be designed to self-assemble and function as the arms (or girders) of a lattice or periodic array. However, the design of the hubs, or the junctions from which multiple DNA sequences radiate, remains a challenge. A series of reports describe the use of immobile branched DNA<sup>3–5</sup> to assemble DNA junctions; this design is based upon biological DNA recombination intermediates. To date, studies involving solely DNA for lattice assembly have been limited to defined polyhedral connectivities<sup>6,7</sup> and two-dimensional arrays.<sup>8</sup>

DNA sequences can also be tethered to various organic linkers, including very simple linear spacers<sup>9</sup> that accommodate two strands of DNA; a simple branched version of methane, tris(hydroxypropyl)aminomethane,<sup>10</sup> that accommodates three strands of DNA; or more complex linkers<sup>11,12</sup> that permit the development of DNA dendrimers. Rigidity has been suggested to be an important component of such building blocks<sup>1,2</sup> for their self-assembly properties. Aromatic acetylenes<sup>13</sup> and aromatic butadienes<sup>14</sup> have both been designed as less flexible linkers to which two DNA strands can be attached. In the former study, various-sized “DNA cycles” were assembled, resulting in circular hybridization products of varying sizes, while in the latter study linear polymers were prepared.

A number of studies have used gold<sup>15–17</sup> or cadmium<sup>18</sup> nanoparticles as hubs to which multiple DNA sequences are attached. While sequence complementarity permits the formation of supramolecular assemblies of these metal nanoparticles,<sup>15</sup> and in the case of gold, with attendant color changes to monitor

\* Corresponding author: Tel 617-552-3622; fax 617-552-2705.

(1) Seeman, N. C. *Angew. Chem., Int. Ed.* **1998**, *37*, 3220–3238.  
(2) Seeman, N. C. *Biochemistry* **2003**, *42*, 7259–7269.  
(3) Kallenbach, N. R.; Ma, R.-I.; Seeman, N. C. *Nature* **1983**, *305*, 829–831.  
(4) Ma, R.-I.; Kallenbach, N. R.; Sheardy, R. D.; Petrillo, M. L.; Seeman, N. C. *Nucleic Acids Res.* **1986**, *14*, 9745–9753.  
(5) Petrillo, M. L.; Newton, C. J.; Cunningham, R. P.; Ma, R.-I.; Kallenbach, N. R.; Seeman, N. C. *Biopolymers* **1988**, *27*, 1337–1352.  
(6) Chen, J.; Seeman, N. C. *Nature* **1991**, *350*, 631–633.

(7) Zhang, Y.; Seeman, N. C. *J. Am. Chem. Soc.* **1994**, *116*, 1661–1669.  
(8) Winfree, E.; Liu, F. R.; Wenzler, L. A.; Seeman, N. C. *Nature* **1998**, *394*, 539–544.  
(9) Fogleman, E. A.; Yount, W. C.; Xu, J.; Craig, S. L. *Angew. Chem., Int. Ed.* **2002**, *41*, 4026–4028.  
(10) Scheffler, M.; Dorenbeck, A.; Jordan, S.; Wustefeld, M.; von Kiedrowski, G. *Angew. Chem., Int. Ed.* **1999**, *111*, 3514–3518.  
(11) Shchepinov, M. S.; Udalova, I. A.; Bridgman, A. J.; Southern, E. M. *Nucleic Acids Res.* **1997**, *25*, 4447–4454.  
(12) Shchepinov, M. S.; Mir, K. U.; Elder, J. K.; Frank-Kamenetskii, M. D.; Southern, E. M. *Nucleic Acids Res.* **1999**, *27*, 3035–3041.  
(13) Shi, J.; Bergstrom, D. E. *Angew. Chem., Int. Ed. Engl.* **1997**, *36*, 111–113.  
(14) Waybright, S. M.; Singleton, C. P.; Wachter, K.; Murphy, C. J.; Bunz, U. H. F. *J. Am. Chem. Soc.* **2001**, *123*, 1828–1833.  
(15) Elghanian, R.; Storhoff, J. J.; Mucic, R. C.; Letsinger, R. L.; Mirkin, C. A. *Science* **1997**, *277*, 1078–1080.  
(16) Mucic, R. C.; Storhoff, J. J.; Mirkin, C. A.; Letsinger, R. L. *J. Am. Chem. Soc.* **1998**, *120*, 12674–12675.  
(17) Storhoff, J. J.; Elghanian, R.; Mucic, R. C.; Mirkin, C. A.; Letsinger, R. L. *J. Am. Chem. Soc.* **1998**, *120*, 1959–1964.  
(18) Niemeyer, C. M.; Burger, W.; Peplies, J. *Angew. Chem., Int. Ed.* **1998**, *37*, 2265–2268.

hybridization events,<sup>19</sup> it is not clear that the nanoparticle–DNA monomers or the subsequent nanoparticle aggregates have the necessary defined and repeating structures that could be used in the assembly of ordered systems. On the other hand, metal–ligand complexes have the advantage of precise three-dimensional geometric shapes; tethering DNA sequences to specific sites on a metal–ligand complex could provide a well-defined geometric monomer for use in the assembly of a repeating periodic array of DNA helices and metal centers. Mesoscale lattices of varying compositions and dimensions could then result simply from the choice of DNA sequence and its length. Sequence complementarity and sequence length are also the defining parameters for the requisite self-assembly of the monomeric building blocks into a supramolecular structure. Relatively few studies<sup>14,20–23</sup> have been reported in which metal–ligand complexes have been used to tether DNA sequences, and in those studies, the metal center generally tethers just two sequences of DNA. Such building blocks could in principle be used for the assembly of linear arrays, but achieving higher-order assemblies such as those based upon a tetrahedral orientation of DNA sequences will require building blocks with four DNA arms.

We describe here the first preparation of multiarm DNA–metal-centered monomers, composed of a Ni(II)–cyclam hub tethering four DNA sequences, and hybridization studies that suggest these complexes can function as monomers for the generation of supramolecular assemblies.

## Experimental Section

Reagents and solvents were from Aldrich (St. Louis, MO), Strem Chemicals (Newburyport, MA), and Lancaster (Windham, NH). Thin-layer chromatography was performed on aluminum-backed precoated aluminum oxide 60 F<sub>254</sub> neutral plates from EM Science (Gibbstown, NJ). Preparative chromatography was performed on aluminum oxide, activated, neutral, Brockmann I standard grade from Aldrich and alumina G-F preparative plates from Analtech (Newark, DE). <sup>1</sup>H NMR spectra were obtained on 300 and 400 MHz Varian multiprobe spectrometers. High-resolution electrospray mass spectroscopy was performed on a Micromass LCT system. MALDI-TOF mass spectroscopy was performed on a Micromass TOF Spec 2E system.

Oligonucleotides were synthesized on an Applied Biosystems 394 DNA/RNA synthesizer (Foster City, CA). DNA synthesis-grade acetonitrile was purchased from Burdick and Johnson (Muskegon, MI). DNA synthesis reagents, 3'-cyanoethyl (CE) phosphoramidites and 5'-CE phosphoramidites, were obtained from Glen Research (Sterling, VA). The 1000 Å CPG supports tethering nucleosides at their 5'-termini (3'-DMT) came from Biosearch Technologies (Foster City, CA).

High-performance liquid chromatography was performed on a Waters 600E multisolvent delivery system equipped with a Waters 2487 dual-wavelength absorbance detector (Milford, MA). Purification was performed on a 4.6 mm/100 mm PEEK column containing POROS oligo R3 reverse-phase support purchased from Applied Biosystems (Foster City, CA). HPLC-grade acetonitrile was obtained from Fisher Scientific (Fair Lawn, NJ).

Concentration of samples was determined by UV–vis measurements performed on a Beckman DU640B spectrophotometer (Fullerton, CA). Thermal denaturation studies were conducted on an Aviv 14DS spectrophotometer equipped with digital temperature control (Lake-wood, NJ). Agarose, acrylamide, and [ $\gamma$ -<sup>32</sup>]ATP were purchased from ICN (Aurora, OH). Polyacrylamide gel electrophoresis (PAGE) was carried out on an apparatus from Hoefer Scientific. Agarose gel electrophoresis was performed on a Sub-cell GT system purchased from Bio-Rad (Hercules, CA). Ethidium bromide and the 20 base pair standard were obtained from Sigma (St. Louis, MO). Imaging of PAGE and agarose gels was conducted on a Bio-Rad Molecular Imager FX system equipped with Quantity One software.

MALDI-TOF mass spectrometry data for metal complex–DNA conjugates were obtained from the Mass Spectrometry Laboratory, School of Chemical Sciences, University of Illinois at Champaign–Urbana, Urbana, IL.

**Synthesis of Cyclam Complex 4.** To 2.18 g (3.77 mmol) of 1,4,8,11-tetraazacyclotetradecane-1,4,8,11-tetraacetic acid tetrahydrochloride hydrate (**1**) in 200 mL of anhydrous dimethylformamide (DMF) was added diisopropylethylamine until a clear solution was obtained. After the solution was cooled to 0 °C, 4.67 g (22.6 mmol) of 1,3-dicyclohexylcarbodiimide and 3.05 g (22.6 mmol) of 1-hydroxybenzotriazole were added, and the mixture was stirred under nitrogen for 3 h. A solution of 6.33 g (15.1 mmol) of 6-dimethoxytrityloxy-1-hexylamine<sup>24,25</sup> in 100 mL of anhydrous DMF was then added dropwise. The reaction was allowed to proceed at ambient temperature overnight and was then analyzed by TLC on alumina (2.5% methanol in dichloromethane). Upon completion (~16 h), the reaction mixture was concentrated to dryness, taken up in CH<sub>2</sub>Cl<sub>2</sub>, washed with saturated sodium bicarbonate solution, dried over sodium sulfate, and evaporated to yield a yellow-brown oil. Purification on alumina eluting with a 0–1.5% methanol gradient in CH<sub>2</sub>Cl<sub>2</sub> yielded 3.6 g (47%) of the fully DMT-protected ligand **2** as a pale yellow oil that formed a white foam when placed under high vacuum. *R*<sub>f</sub>(2.5% methanol in CH<sub>2</sub>Cl<sub>2</sub>) = 0.75. <sup>1</sup>H NMR (CDCl<sub>3</sub>, 400 MHz):  $\delta$  1.00–1.90 (m, 32H, -CH<sub>2</sub>-), 1.90 (m, 4H, cyclam -CH<sub>2</sub>-), 2.57 (m, 16H, cyclam -CH<sub>2</sub>-N), 3.00 (m, 16H, N-CH<sub>2</sub>-CO, -CH<sub>2</sub>-ODMT), 3.10 (m, 8H, amide -CH<sub>2</sub>-), 3.79 (s, 24H, -OCH<sub>3</sub>), 6.80 (d, 16H, Ar-H), 6.90 (t, 4H, CONH), 7.10–7.50 (m, 36H, Ar-H). MALDI-TOF MS: calculated 2038.63, observed 2039.20.

The tris-DMT compound **3** was prepared by dissolving 1.0 g (0.49 mmol) of **2** in 100 mL of CH<sub>2</sub>Cl<sub>2</sub>, to which a 3% solution of dichloroacetic acid in CH<sub>2</sub>Cl<sub>2</sub> was added dropwise with stirring. The reaction was closely monitored by TLC on alumina (5% methanol in CH<sub>2</sub>Cl<sub>2</sub>). When the reaction appeared to start to progress beyond the removal of one DMT protecting group, it was quenched by the addition of saturated sodium bicarbonate solution. Additional CH<sub>2</sub>Cl<sub>2</sub> was added and the mixture was washed with saturated sodium bicarbonate, dried over sodium sulfate, and evaporated to a dark yellow oil. Purification on an alumina column eluting with a 1–2.5% methanol in CH<sub>2</sub>Cl<sub>2</sub> gradient yielded recovered starting material (~0.75 g) and 0.197 g of **3**, a white foam after it was placed under high vacuum. *R*<sub>f</sub>(5% methanol in CH<sub>2</sub>Cl<sub>2</sub>) = 0.81. <sup>1</sup>H NMR (CDCl<sub>3</sub>, 400 MHz):  $\delta$  1.20–1.90 (m, 36H, OCH<sub>2</sub>-, cyclam -CH<sub>2</sub>-), 2.58 (m, 16H, cyclam -CH<sub>2</sub>-N), 3.00 (m, 14H, N-CH<sub>2</sub>-CO, -CH<sub>2</sub>-ODMT), 3.10 (m, 8H, amide -CH<sub>2</sub>-), 3.60 (t, 2H, -CH-OH), 3.78 (s, 18H, -OCH<sub>3</sub>), 6.80 (d, 12H, Ar-H), 6.90 (t, 4H, CONH), 7.10–7.50 (m, 27H, Ar-H). MALDI-TOF MS: calculated 1736.26, observed 1740.00 (M + 4H<sup>+</sup>).

To incorporate the Ni(II) cation, 0.150 g (0.086 mmol) of **3** and 0.031 g (0.17 mmol) of nickel(II) acetate were dissolved in 10 mL of ethanol and heated to reflux. After refluxing overnight, excess NH<sub>4</sub>PF<sub>6</sub> was added and allowed to stir briefly. The reaction was cooled

(19) Mirkin, C. A.; Letsinger, R. L.; Mucic, R. C.; Storhoff, J. J. *Nature* **1996**, *382*, 607–609.

(20) Wiederholt, K.; McLaughlin, L. W. *Nucleic Acids Res.* **1999**, *27*, 2487–2493.

(21) Lewis, F. D.; Helvoigt, S. A.; Letsinger, R. L. *J. Chem. Soc., Chem. Commun.* **1999**, 327–328.

(22) Vargas-Baca, I.; Mitra, D.; Zulyniak, H. J.; Banerjee, J.; Sleiman, H. *Angew. Chem., Int. Ed.* **2001**, *40*, 4629–4632.

(23) Stewart, K. M.; McLaughlin, L. W. *J. Chem. Soc., Chem. Commun.* **2003**, 2934–2935.

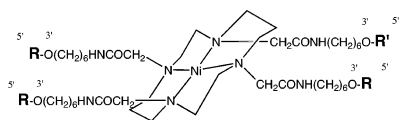
(24) Jackson, D. S.; Fraser, S. A.; Ni, L.-M.; Kam, C.-M.; Winkler, U.; Johnson, D. A.; Froelich, C. J.; Hudig, D.; Powers, J. C. *J. Med. Chem.* **1998**, *41*, 2289–2301.

(25) Avino, A.; Guimil Garcia, R.; Albericio, F.; Mann, M.; Wilm, M.; Neubauer, G.; Eritja, R. *Bioorg. Med. Chem.* **1996**, *4*, 1649–1658.

to ambient temperature and excess  $\text{CH}_2\text{Cl}_2$  was added. After standard workup procedures, solvent removal yielded a pale purple oil (**4**) soluble in acetonitrile. MALDI-TOF MS: expected 1794.96, observed 1796.0 ( $\text{M} + \text{H}^+$ ). Visible spectroscopy (acetonitrile)  $\lambda_{\text{max}} = 565 \text{ nm}$ .

**DNA Synthesis.** The initial DNA sequence was synthesized on a 1  $\mu\text{M}$  scale on 1000 Å 5'-linked support by use of 5'-CE phosphoramidites obtained from Glen Research (Sterling, VA). The "reverse coupling" technique was then employed to attach **4** to the initially synthesized 5' → 3' strand. Two syringes were attached to either end of the synthesis column: one contained 200  $\mu\text{L}$  of 2-(cyanoethyl)tetraisopropylphosphorodiamidite, and the second contained 200  $\mu\text{L}$  of the tetrazole activator solution. After the reagents were mixed in the column, the column was placed on a shaker platform and phosphitylation was allowed to occur for 2 h. After the column was washed with acetonitrile, two syringes, one containing 20 mg of **4** in 100  $\mu\text{L}$  of acetonitrile and the second containing 150  $\mu\text{L}$  of tetrazole activator solution, were used to mix the reagents in the column. After a 120 min reaction time, capping and oxidation were performed, and the synthesis of the remaining three DNA arms in the 3' → 5' direction was performed on the synthesizer with conventional phosphoramidites. Deprotection of the DNA was conducted in the conventional manner. Conjugates were purified by 10% denaturing polyacrylamide gel electrophoresis (PAGE), recovered by elutrap, and desalted on disposable Econo-pac G10 columns (Bio-Rad). Yields varied from 5 to 10  $\text{A}_{260}$  units.

MALDI-TOF analyses:



Complex	Sequences	Calculated	Observed	
5	R = R' = 5'-TCGACTCGACCAGCTCAGTp-3'	25,287.65	25,292.48	
6	R = R' = 5'-AGCTGAGCTGGTCGAGTCGAp-3'	25,928.05	25,973.78	(M + 2Na)
7	R = 5'-GATCAGCGGTGGCGACTAGp-3'	25,767.95	25,768.43	
	R' = 5'-TCGACTCGACCAGCTCAGTp-3'			

**Hybridization Experiments.** Conjugates were radiolabeled with end-labeling-grade [ $\gamma$ - $^{32}\text{P}$ ]ATP and T4 polynucleotide kinase in 50 mM Tris-HCl, pH 7.6, 10 mM  $\text{MgCl}_2$ , and 10 mM 2-mercaptoethanol at 37 °C for 2 h. The radiolabeled conjugates were then desalted on a Sep-Pak column and lyophilized to dryness. For the hybridization studies, individual samples were prepared by adding the required amount of conjugate and complement to an eppendorf tube and drying by speed vac. To the residue was added 5  $\mu\text{L}$  of 80 mM Tris-borate-EDTA buffer (TBE), pH 8.3. Samples were heated for 2 min at 95 °C and allowed to cool gradually to ambient temperature. After cooling, 5  $\mu\text{L}$  of Ficoll loading buffer containing TBE and tracking dyes was added to each sample. Samples were loaded onto 19:1 cross-linked 10% nondenaturing gels and were developed in a TBE buffer system at 200 V for 8–10 h. Larger complexes were analyzed by electrophoresis in 2.5% agarose gels and complexes were visualized by ethidium bromide staining. Some agarose gels were developed in TBE buffer, while others employed Tris-borate with 1 mM  $\text{MgCl}_2$ .

Radiolabeling of each complex followed by PAGE analysis resulted in single bands, although with anomalous mobilities relative to a 20 base pair ladder. The migration anomalies are likely in part due to the presence of the Ni(II) complex and in part due to the orientation of the sequences. Migration anomalies were determined by comparison of the apparent lengths of various DNA Ni(II)-cyclam complexes relative to a standard 20 bp ladder of standard duplexes differing in sizes by 20 bp versus the actual length of the complexes. Migration anomalies are reported as the ratio of the apparent length divided by the known sequence length.

## Results and Discussion

We have designed hubs for the purpose of tethering multiple DNA sequences, and in the present study we have employed a

cyclic ligand in this role. The use of a metal ion in this context is not essential to the underlying lattice concept, but the metal ion will serve to constrain the central hub and may result in better overall organization of the structure. "Rigidity" or "stiffness" is a characteristic of monomer building blocks thought<sup>2</sup> to be critical to produce well-structured DNA-based arrays. In related examples, where the ligand is not cyclic in nature,<sup>22,23</sup> the metal is a key element in defining the geometry of the central hub.

The construction of a tetrahedral lattice from hubs bearing single-stranded DNA requires that every hub in the lattice be bound to four DNA sequences. In the present study we have used a Ni(II)-1,4,8,11-tetraazacyclotetradecane (cyclam) complex to which four DNA arms are attached (Scheme 1). In the described design, the choice of sequences for the DNA arms of the building block is quite general. Two building blocks, each with four identical sequences of uniform polarity, were prepared such that the sequences of one building block were complementary to the second. Mixing samples of the two monomers should result in self-assembly of higher-order structures.

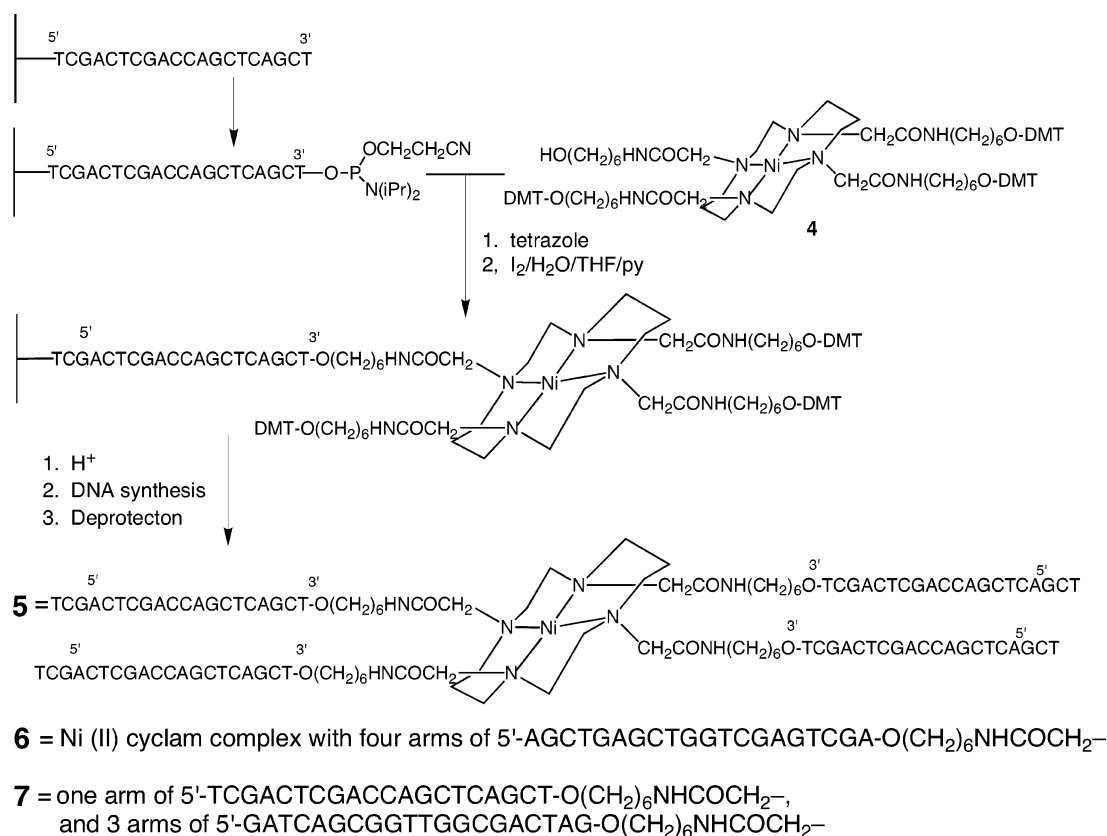
Model studies suggested that a simple linker between the DNA and the metal center was necessary to properly position the four DNA arms and minimize steric crowding. Charge-charge repulsion effects should result in a largely tetrahedral orientation of the DNA arms, and these interactions may additionally impart some stiffness to the monomers, even though the linkers are simple and flexible carbon chains. Synthesis of the monomer began with attachment of the DMT-protected linkers to cyclam tetraacetic acid. One DMT group was removed by a limited acid hydrolysis, and insertion of the Ni(II) metal ion afforded compound **4** (Scheme 1). Control experiments indicated that the Ni(II) complex was stable to the conditions of DNA synthesis and deprotection. Assembly of the desired monomer employed a reverse coupling protocol<sup>26</sup> in which the terminal nucleoside of the support-bound oligonucleotide was phosphitylated (Scheme 1) and subsequently **4** was added in the presence of tetrazole. To achieve uniform sequence orientation, the initial DNA synthesis was performed in the 5' to 3' direction with reverse nucleoside phosphoramidites<sup>27</sup> (3'-DMT, 5'-phosphoramidite). After incorporation of the cyclam complex by the reverse coupling reaction (Scheme 1), the remaining linkers were elongated by conventional DNA synthesis. The final product was a nickel-centered cyclam complex tethering four DNA sequences of identical length (20-mers) and polarity (see complexes **5–7**). After deprotection, the products were isolated by PAGE. In addition to gel analyses to determine purity, MALDI-TOF mass spectra were obtained for product identification. The MALDI-TOF mass spectra indicated peaks for the parent complexes (see Experimental Section) and confirmed that after PAGE isolation in the presence of  $\text{Na}_2\text{EDTA}$  there was no loss of nickel cation.

After radiolabeling, the complexes migrated as single species by electrophoresis with sequence lengths of at least 80 nucleotides (see migration anomaly below). To further confirm that the presence  $\text{Na}_2\text{EDTA}$  in the gel buffer did not result in extraction of the Ni(II) cation, we incubated a sample of the ligand in methanol/water containing  $5 \times$  TBE gel buffer (5 mM

(26) Rajur, S. B.; Robles, J.; Wiederholt, K.; Kuimelis, R. W.; McLaughlin, L. W. *J. Org. Chem.* **1997**, *62*, 523–529.

(27) Horne, D. A.; Dervan, P. B. *J. Am. Chem. Soc.* **1990**, *112*, 2435–2437.

Scheme 1



Na<sub>2</sub>EDTA) at ambient temperature overnight. MALDI-TOF analysis indicated that the Ni–cyclam complex remained intact. In a second experiment, the same reaction was performed at 55 °C. Under these harsher conditions, it required in excess of 18 h to extract approximately 50% of the Ni from the cyclam ligand.

With metals in the central hubs of the designed complexes, supramolecular assemblies should result in periodic spacing of the metal centers. This arrangement of metals may be valuable for analyses of such assemblies, particularly those based upon X-ray diffraction methods. The metals will serve as bright sites of diffraction that should be easy to locate in the resulting diffraction patterns and will aid in determining whether the higher-order assemblies adopt any periodic organization. On the other hand, metals are known to interact with DNA through a variety of mechanisms including coordination, hydrolysis, ligand binding, and redox processes. In some cases these reactions could effectively interfere with DNA hybridization. For example, cis-dichloroplatinum complexes bind d(GpG) very effectively<sup>28</sup> in both single-stranded and double-stranded DNA through the N7 nitrogens,<sup>29</sup> and it has long been known that Zn<sup>2+</sup> and Pb<sup>2+</sup> can effectively hydrolyze RNA sequences.<sup>30</sup> Ruthenium complexes coordinated to planar ligands can bind specific forms of DNA primarily through intercalation of the ligand,<sup>31</sup> and a variety of metal complexes including those coordinated to copper,<sup>32</sup> iron,<sup>33</sup> and ruthenium<sup>34</sup> through redox processes can

generate reactive species such as hydroxyl radicals that can cleave the DNA backbone. For the present study we chose Ni(II)–cyclam for the central hub principally because it is known to be relatively inert with respect to these various types of interactions. It has been reported that the parent compound Ni(II)–cyclam can be oxidized to the Ni(III) complex in the presence of peracid.<sup>35</sup> The Ni(III) complex results in cleavage of DNA at dG sites, presumably by electron abstraction from guanine residues while the cyclam complex returns to the inert Ni(II) state. The intermediacy of 8-oxo-2'-deoxyguanosine in these reactions remains unconfirmed. Despite this reported activity, Ni(II)–cyclam complexes are more or less inert under the present conditions and seemed a reasonable choice for a structural role in the monomers described here.

Although the cyclam nitrogens that tether the linker/DNA sequences are oriented with a more or less square planar geometry, the presence of the flexible linkers and charge–charge repulsion effects between strands should dictate a largely tetrahedral orientation of the DNA sequences; hybridization to form four DNA duplexes at four positions around the cyclam ligand should reinforce that geometry. To determine the thermal stability of DNA duplexes tethered to a Ni(II)–cyclam complex, we prepared complex **5** fully hybridized to its complementary 20-mer. It exhibited a single *A*<sub>260</sub> vs temperature transition with a midpoint of 73.3 °C. For the simple cyclam-free 20-mer duplex, the *T*<sub>m</sub> value was nearly identical at 73.8 °C (plots available in Supporting Information). Additionally, to confirm that each hub contained four DNA arms available for hybridiza-

(28) Sherman, S. E.; Gisbson, D.; Wang, A. H.-J.; Lippard, S. J. *J. Am. Chem. Soc.* **1988**, *110*, 7368–7381.

(29) Ohndorf, U.-M.; Rould, M. A.; He, Q.; Pabo, C. O.; Lippard, S. J. *Nature* **1999**, *399*, 708–712.

(30) Eichhorn, G. L.; Shin, Y. A. *J. Am. Chem. Soc.* **1968**, *90*, 7322–7327.

(31) Barton, J. K. *Science* **1986**, *233*, 727–729.

(32) Pope, L. E.; Sigman, D. S. *Proc. Natl. Acad. U.S.A.* **1984**, *81*, 3–7.

(33) Tullius, T. D. *Curr. Opin. Struct. Biol.* **1991**, *1*, 428–434.

(34) Sitali, A. *J. Am. Chem. Soc.* **1992**, *114*, 2303–2304.

(35) Muller, J. G.; Chen, X.; Dadiz, A. C.; Rokita, S. E.; Burrows, C. J. *J. Am. Chem. Soc.* **1993**, *65*, 545–550.

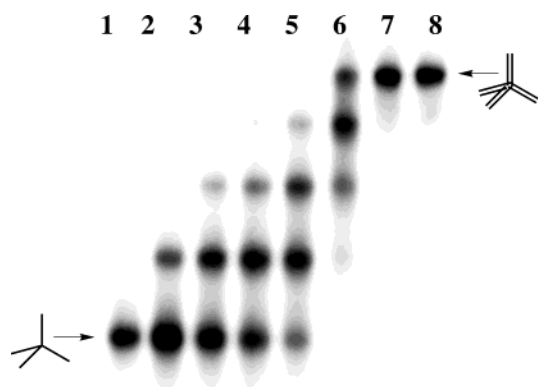


**Figure 1.** Nondenaturing PAGE analysis, 10% acrylamide and 0.5% bisacrylamide,  $1\times$  TBE, pH 8.3, of hybridizations performed in the gel buffer between the Ni-cyclam complex **5** containing four identical DNA arms and the complementary 20-mer. Lane 1: [ $^{32}\text{P}$ ]-radiolabeled Ni-cyclam **5** of Scheme 1 with four single-stranded DNA arms. Lanes 2–7: Ni-cyclam complex **5** after addition of 0.25, 0.5, 1, 2, 3, and 4 equiv, respectively, of 5'-d(AGCTGAGCTGGTCGAGTCGA). Lane 8: 8-fold excess of complementary 20-mer.

tions to complementary sequences, we titrated monomer **5** with increasing amounts of the simple complementary 20-mer. As the concentration of the 20-mer increased, we observed a series of four hybridization products with stepwise decreases in mobility (Figure 1). The observation that no radioactive hybridization products were observed between steps indicates that no monomers containing partial arms were present. Furthermore, the observation that all of the initially radiolabeled material could be shifted to the fourth hybridization product of lowest mobility indicates that all of the prepared material contained four DNA arms, and the observation that upon addition of excess 20-mer no additional hybridization products were present indicates the absence of any nonspecific hybridization. This experiment shows that all four arms of the metal center are available for hybridization to complementary sequences and that the stability of the central hub tethering four DNA duplexes is essentially the same as an isolated duplex; the presence of the conjugated Ni(II)-cyclam does not result in duplex destabilization.

The hybridization products of Figure 1 migrated anomalously relative to a standard 20-bp ladder (the standard ladder was visualized by fluorescent staining and is not visible in the autoradiogram of Figure 1). We have reported the anomalies as the apparent migration lengths divided by the known sequence lengths (Table 1). For the single-stranded complex (**5**), the migration anomaly (1.3) reflects that the complex with 80 nucleotides (four 20-mer arms) migrates with an apparent length of 104 nucleotides. This is a relative minor migration anomaly that can be explained in part from the presence of the positively charged Ni(II) as well as the additional mass of the cyclam ligand and four linkers present in the complex. However, after the addition of the first complementary 20-mer, the complex size or sequence length increases by only another 20 residues, but the apparent length increases by 40 residues. Similarly, the addition of the second, third, and fourth complementary 20-mers results in actual sequence lengths of 120, 140, and 160 nucleotides, respectively. In this series, the apparent lengths are 196, 256, and 330 nucleotides, reflecting migration anomalies

**Table 1.** Migration Anomaly for Ni-Cyclam Complexes Tethering Four DNA Sequences

duplex arms	0	1	2	3	4
sequence length	80	100	120	140	160
apparent length <sup>a</sup>	104	144	196	256	330
migration anomaly <sup>b</sup>	1.3	1.44	1.63	1.82	2.06

<sup>a</sup> Apparent length relative to a 20 bp standard ladder. <sup>b</sup> Migration anomaly = apparent length/sequence length in a 10% acrylamide gel with cross-linking of 19:1.

of 1.63, 1.82, and 2.06, respectively. These stepwise increases in the observed migration anomalies suggest that as more of the single-stranded DNA arms are converted to duplexes, the complex experiences more difficulty in migrating through the pores of the gel. The increase in the migration anomaly results from the increase in the number of nucleotide arms or their positions, not simply from the additional mass of the hybridized arms.

Our understanding of the migration of DNA in polyacrylamide gels is based upon the Ogstron model<sup>36–38</sup> or on tube reptation ideas,<sup>39,40</sup> both of which are dependent upon the entanglement properties of the gel matrix. In the former, the gel is a random mesh with variations in pore sizes. Electrophoretic mobility is obtained as the product of the free solution mobility and an exponential function of the cross-sectional area of the polyion divided by the mesh size. In the reptation model, the gel fibers impose a sideways constraint on the DNA and it migrates snakelike through tubelike regions. For a given gel concentration, decreases in electrophoretic mobility will be largely correlated with increases in the cross-sectional area of the polyion. The larger cross-sectional area limits movement through the gel as described by either model. Thus, the increases in the migration anomaly values observed for the present complexes suggest an increase in cross-sectional area and the presence of a more extended “starlike” shape, particularly for the fully hybridized monomers. A tetrahedral orientation for four DNA arms provides the optimal extended starlike conformation, and this orientation also minimizes charge–charge repulsion effects between hybridized arms. The observed migration anomalies for these complexes suggest that even with the presence of the flexible linkers, the complexes, particularly when fully hybridized, are more extended and may be more rigid than would otherwise be expected.

To prepare high molecular weight assemblies by self-assembly of complementary Ni(II)-cyclam monomers, it is necessary to show that two or more monomers can hybridize together and form higher-order structures (Figure 2). Toward this end, two types of hybridization assembly experiments were performed

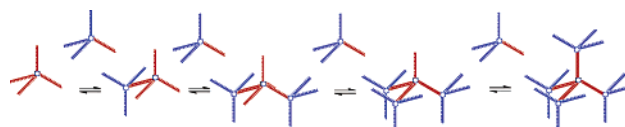


**Figure 2.** Illustration of the hybridization equilibrium between complex **6** containing four identical sequence arms (all illustrated in red) and complex **7** containing one arm complementary to those of **6** and three arms not complementary (illustrated with one red arm and three blue arms).

- (36) Ogstron, A. G. *Trans. Faraday Soc.* **1958**, *54*, 1754–1757.  
 (37) Chrambach, A.; Rodbard, D. *Science* **1971**, *172*, 440–451.  
 (38) Cobbs, G. *Biophys. J.* **1981**, *35*, 535–542.  
 (39) Levine, S. D.; Zimm, B. H. *Science* **1989**, *245*, 396–399.  
 (40) Perkins, T. T.; Smith, D. E.; Chu, S. *Science* **1994**, *264*, 819–822.

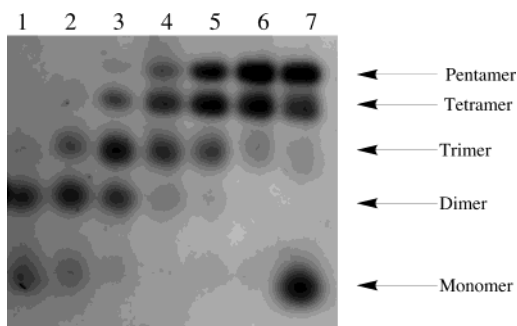


**Figure 3.** Hybridization experiment involving Ni-cyclam complex **6** with four identical 20-mer arms analyzed by electrophoresis in a 2.5% agarose gel. Lanes 1–7 contain a fixed quantity of complex **6** and increasing amounts of complex **7** (having one complementary arm) in 25 mM PIPES, pH 7.0, 10 mM Mg<sup>2+</sup>, and 50 mM NaCl. Lanes 1–7 contain 0.5, 1, 2, 3, 4, 5, and 10 equiv of complex **7**.

for monomers **5**–**7**. In one case we examined the hybridization of **6** with **7** (**7** contains one arm complementary to those of **6** and three arms that are not complementary). Hybridization of these monomers should result in a largely defined and tetrahedral assembly: **6** surrounded by 4 equivalents of **7** (see Figure 2). As aliquots of **7** were added to **6** in a low-salt (25 mM PIPES, pH 7.0, 50 mM NaCl, and 10 mM MgCl<sub>2</sub>) solution, agarose gel electrophoresis indicated a series of hybridization products (similar to those of Figure 1), each with a stepwise reduction in gel mobility (Figure 3). As expected, the final hybridization step to convert the tetramer (three hybridization events) to the pentamer (four hybridization events) was the most difficult, presumably because pentamer formation occurs with the maximum charge–charge repulsion effects between unhybridized arms. Each assembly event in the formation of the pentamer benefits from the hybridization of a single 20-mer duplex, but each assembly event is also affected by charge–charge repulsion from the three additional tethered and nonhybridized sequences. Counterion effects can be expected to modulate the repulsion effects as achieved by increases in the salt concentration of the buffer solution (data not shown). When higher concentrations of divalent metal ion were used in addition to NaCl (e.g., 100 mM Mg<sup>2+</sup>), all of **6** could be converted to the fully hybridized (slower migrating) pentamer complex (see Supporting Information). The success in forming the pentamer complex, in which each building block must overcome the charge–charge repulsion effects from multiple nonhybridizing arms while complex formation is the consequence of hybridization by a single arm, suggests that higher-order complexes involving hybridization events with multiple arms of each building block should be possible, and even preferable since assemblies with the greatest number of hybridization events will likely be the most stable form of the monomers.

In a second experiment we examined hybridization between the two monomers **5** and **6**, each having four identical arms complementary to each other. Hybridization events involving multiple arms from both **5** and **6** are now possible. Figure 4 illustrates the hybridization experiment between various quantities of complexes **5** and **6**. Complexes **5** and **6** each have four identical DNA arms, and the sequences of complexes **5** and **6** are complementary to each other (but not self-complementary). With a ratio of complex **5**:complex **6** of 4:1 (lane 1), the resulting products consist mostly of relatively small assemblies, largely monomers, dimers, and trimers with some larger

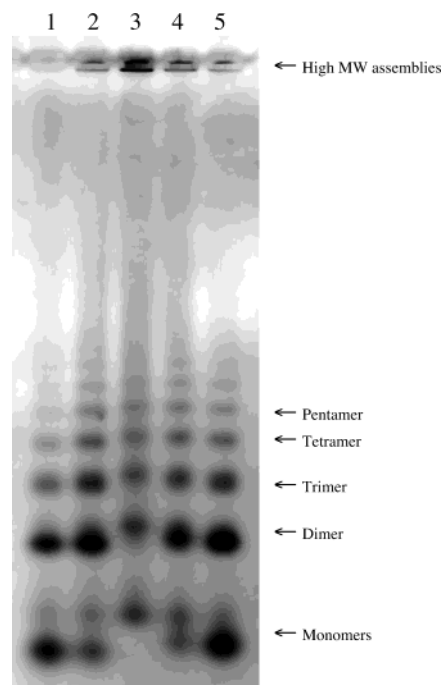


**Figure 4.** Hybridization experiment involving Ni-cyclam complex **5** with four identical 20-mer arms and complex **6** with four identical 20-mer arms that are complementary to the sequences of complex **5** analyzed by electrophoresis in a 2.5% agarose gel. Ratios of complex **5** to complex **6** were as follows: lane 1, 4:1; lane 2, 2:1; lane 3, 1:1; lane 4, 1:2; lane 5, 1:4. Hybridization was performed in 25 mM PIPES, pH 7.0, 10 mM Mg<sup>2+</sup>, 0.5 mM spermine, and 50 mM NaCl.

assemblies. With a **5**:**6** ratio of 2:1 (lane 2), the monomer is largely absent. There are some smaller assemblies still present, but high molecular weight materials have begun to appear in the gel wells at the top of the figure. With a **5**:**6** ratios of 1:1 (lane 3), most of the DNA appears in the gel well as high molecular weight assemblies. The remaining two lanes (4 and 5) contain the complementary mixtures of complexes **5** and **6** at the reverse ratios (1:2 and 1:4) and result in comparative patterns. The observation that, after the assembly of 5- or 6-mer complexes, relatively little is visible on the gel other than the high molecular weight assemblies may indicate that the assembly process bears some semblance to crystallization processes, such that after formation of the seed assembly the incorporation of additional monomers is thermodynamically very favorable and then the predominant assemblies are those of high molecular weights.

The high molecular weight assemblies appear to be present in the gels as two bands (Figure 4). This phenomenon results because after addition of the samples to the wells of the horizontal agarose gel, the high molecular weight assemblies appear to coat the front and bottom of the sample wells. What appears to be a separation between two “bands” is the actual width of the sample well. These assemblies do not migrate away from the sample well surfaces and into the gel. After electrophoresis, these materials readily take up ethidium bromide and can be visualized in the conventional manner. Additionally, these assemblies can be easily washed away from the sample well after electrophoresis and ethidium staining with a gentle stream of water from a pipet. Whether this material in the sample wells is a precipitate resulting from multiple hybridization events, a gel-like material, or a type of ordered lattice remains to be determined.

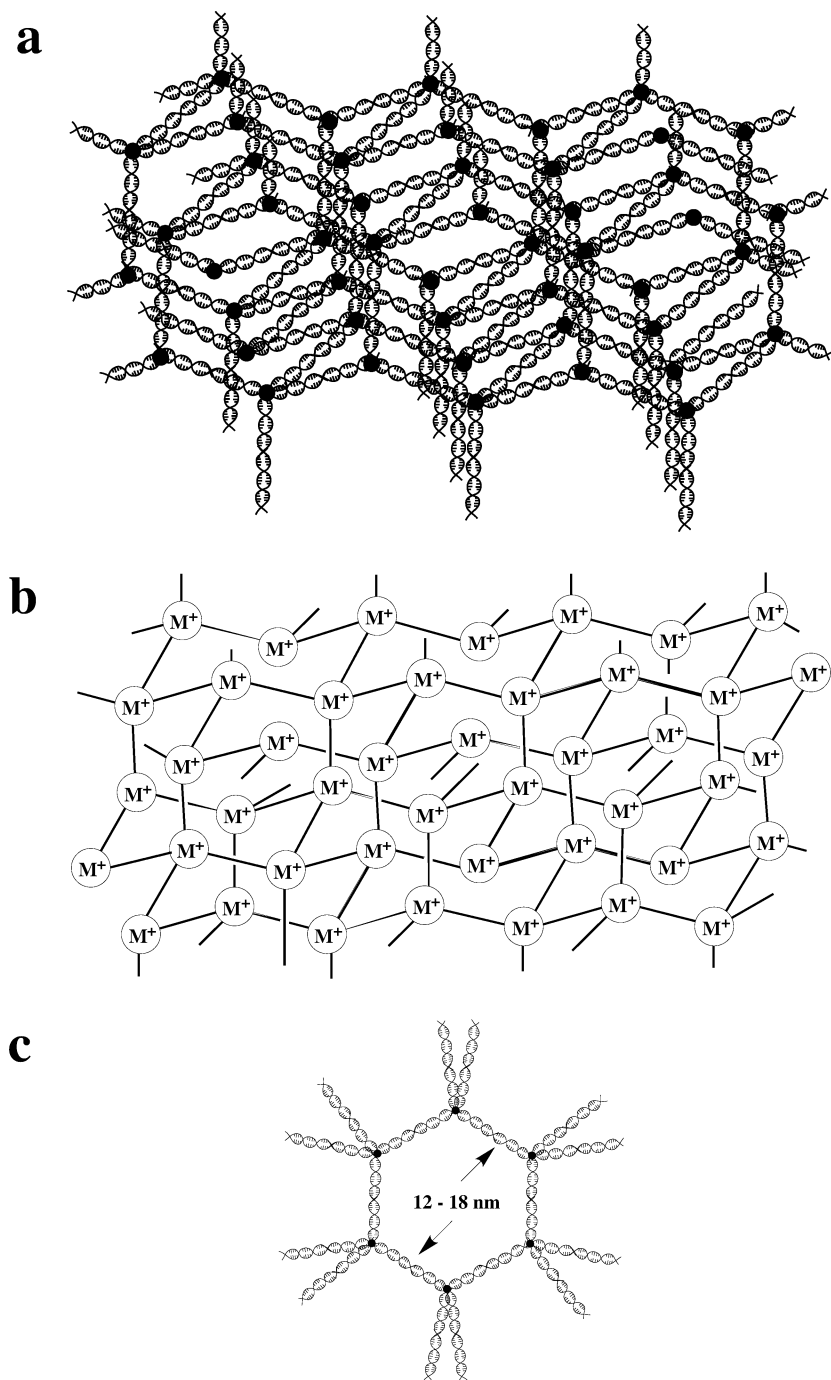


**Figure 5.** DNA–metal hybridization assemblies can be viewed as (a) a latticelike structure of DNA sequences used to bind ligands or protein assemblies for structural analyses, (b) an array of metal complexes potentially valuable for information storage or for their electronic or photoelectric properties, or (c) a material of regular and defined pores of nanometer sizes for the entrapment or controlled release of nanoscale devices or therapeutics.

The monomers present in the gel of Figure 4 migrate through the non-denaturing agarose gel and appear at the bottom of the gel, sometimes with two slightly different mobilities. In the absence of complementary hybridization, this behavior may reflect some variations in conformation that lead to slightly different mobilities. This phenomenon is common but not yet fully understood.

Although relatively large for monomeric building blocks (MW  $\sim$  25 000), the Ni(II)–cyclam DNA complexes described here permit the construction of large assemblies resulting from hybridization. We cannot at this time determine whether these assemblies are periodic in nature or whether there is a signifi-

cant component of linear assembly inherent in the hybridization products. One reason for performing the experiments illustrated in Figure 2 and described in Figure 3 was to determine conditions that would permit all four arms of a monomer to hybridize with four additional monomers. If charge–charge repulsion effects can be minimized, the most stable assembly should be that with maximized hybridization events. For the present monomers, lattice-like assemblies rather than linear hybridization products will tend to maximize the hybridization events.

The resulting assemblies can be viewed from one perspective as arrays of DNA sequences; in the ideal case, a periodic lattice

results (Figure 5a). If these ordered assemblies are amenable to X-ray diffraction analyses, then various guest molecules such as ligands, protein assemblies, or other nucleic acids could use the DNA arms of the lattice as a scaffold, and such assemblies would themselves be amenable to further structural analyses.<sup>2</sup> An alternative view of these materials is that the DNA simply functions as a ruler to precisely position a periodic array of metal centers (Figure 5b), involving the same or two alternating elements. Appropriate choice of the metal center(s) could result in mesostructures having electric or photoelectric properties. The ability to address individual metal centers by redox activity or electronic excitation might make such materials amenable to high-density information storage. An ordered mesoscale lattice assembly would also provide a material having a regular and periodic pore structure with dimensions of nanometers to tens of nanometers, the pore size being defined simply by the length

of the DNA arms used to assemble the lattice (Figure 5c). Such pores could be used to sequester nanoscale guests, possibly viruses, or alternatively, to provide for the controlled release, for example, of nanoscale therapeutics. Such a controlled release would largely be a function of the denaturation of the DNA duplexes that define the pores, a process that should easily be modulated by sequence length/composition and salt concentration at a given temperature.

**Acknowledgment.** This work was supported by a grant from the NIH (GM53201).

**Supporting Information Available:** Experimental figures (PDF). This information is available free of charge via the Internet at <http://pubs.acs.org>.

JA037424O